Inverse Problems 6 (1990) 697–708. Printed in the UK

Estimation of locations of bioelectric sources using an equivalent filter

Thomas G Xydis†, Andrew E Yagle† and Alan H Kadish‡

† Department of Electrical Engineering and Computer Science, The University of Michigan, Ann Arbor, MI 48109-2122, USA

‡ Department of Internal Medicine, The University of Michigan, Ann Arbor, MI 48109-0022, USA

Received 30 January 1990

Abstract. We estimate the number and locations of bioelectric sources in a horizontally layered volume conductor. By modelling the extracellular medium as an equivalent filter, the location estimation problem becomes one of estimating parameters of this equivalent filter, given cursory knowledge of the functional form of the desired sources. The new procedure (1) is computationally efficient, (2) accurately models noise effects on the location estimates, and (3) automatically regularises noisy data. Numerical results are presented, and the Cramer–Rao bound for depth estimation is derived.

1. Introduction

The *location* estimation problem for bioelectric sources can be formulated as follows. Given some knowledge of the functional form of two-dimensional bioelectric sources at unknown locations in a horizontally layered volume conductor with known structure, and measurements of the resulting extracellular field in a plane parallel to the sources, determine the number and locations of any sources present.

This problem is of interest in cardiology. Healthy cardiac muscle consists of multiple active layers. After a myocardial infarction many of the layers are dead. The problem of determining which, if any, layers are still active can be formulated as such a location estimation problem.

Di Persio and Barr [1] presented a solution to a related one-dimensional inverse problem. By utilising a template matching algorithm, they were able to estimate the location of an action potential along a strand. Oostendorp and Oosterom [2] treated the general problem of multiple dipole sources in an arbitrary inhomogeneous medium, but this formulation requires a boundary element integral, resulting in a huge nonlinear least squares problem. And the Gabor–Nelson equations [3] can only be used to find a *single* dipole inside a *homogeneous* volume conductor; our formulation permits multiple sources in inhomogenous (layered) media.

The new method proposed here uses the *medium filter* formulation of [4, 5] to transform the location estimation problem into one of estimating the parameters of an unknown filter. We formulate this as a composite multiple-hypothesis testing problem, which can be solved using an extension of well known procedures in communication theory [6]. This provides numerically efficient solutions of arbitrary source estimation

0266-5611/90/040697+12$03.50

problems, easily handling cases of both single and multiple sources with arbitrary locations and orientations.

In [4, 5] the solution to the two-dimensional volume conductor forward and inverse *source* estimation problems was facilitated by modelling the extracellular media as an equivalent filter. The problem treated there was as follows. Given the location of a bioelectrical source, the structure of the extracellular medium, and potential measurements at the surface of the medium, compute the functional form of the unknown source. Note that in this paper we consider a different problem: given the functional form of the bioelectrical source, the structure of the extracellular medium, and potential measurements at the surface of the medium, compute the location of the unknown source.

Bioelectrical sources have been modelled as current source densities, as in [7], transmembrane potentials, as in [8], and as evoked extracellular potentials, as in [4, 5]. These formulations can be related to each other. Evoked extracellular potentials and transmembrane potentials have been related to current source densities by, among others, the authors of [9, 10]. Linearity of the medium implies that a given source type corresponds to a unique source of each other type, to within an additive constant [8].

This paper uses extracellular potentials in its presentation; current source densities or transmembrane potential source representations can also be used. The only difference is that the medium filter is different for each source type (see the appendices); the medium filters for transmembrane potentials and current densities are obtained from the medium filter for extracellular potentials by multiplication by an additional function (see appendices B and C).

Several numerical examples of the algorithm, using extracellular potentials as source functions in a homogeneous media, are also provided. Estimation of locations and orientations of single and multiple active layers are considered separately. The Cramer–Rao bound for depth estimation of a single active layer is derived and discussed.

2. Problem formulation

2.1. Assumptions

We make the following assumptions, following [5]:

1. The tissue acts as a synctium, so that individual cell contributions to the source functions need not be considered separately. This equivalent cell assumption has been used by many authors [7, 8, 11].

2. The extracellular medium is linear and consists of horizontal, anisotropic, electrically passive layers with known conductivities and thicknesses.

3. The problem is quasistatic, implying that the medium has negligible reactance and propagation delay. Thus all potentials are computed at an instant in time. The quasistatic assumption ensures that each sample will be independent of the other samples [12].

4. All sources can be modelled as two-dimensionally distributed potentials lying in the plane of the layers of the medium. The spatial extent and average amplitude of each source is known; otherwise the sources are unknown.

All of the above assumptions are physiologically reasonable [10], except for the *a priori* knowledge of the extent and average value of each source. This information is needed so that the unknown sources can be matched filtered (see below). However, the effects of the intervening medium must be included. In order to do this, the medium is modelled as an equivalent filter.

Throughout this paper $s(x, y, x', y', z')$ is the two-dimensional source potential. $s(x, y)$ is a known two-dimensional function; (x', y', z') is its unknown translation from the origin. $\phi(x, y, x', y', z')$ represents the observed potential at the surface $z = 0$ of the volume conductor due to $s(x, y, x', y', z')$, and $r(x, y, x', y', z')$ is $\phi(x, y, x', y', z')$ plus white Gaussian noise. Fourier transforms of these quantities are denoted using capital letters, e.g.,

$$S(k_x, k_y, x', y', z') = \mathcal{F}_{x \to k_x} \mathcal{F}_{y \to k_y} \{s(x, y, x', y', z')\}. \tag{1}$$

2.2. Effect of source depth

In [4, 5] it is shown that the observed potential $\phi(x, y, x', y', z')$ is related to the source potential $s(x, y, x', y', z')$ by

$$\begin{aligned} \phi(x, y, x', y', z') &= \mathcal{F}^{-1}_{k_x \to x} \mathcal{F}^{-1}_{k_y \to y} \{S(k_x, k_y, x', y', z') H(k_x, k_y, z')\} \\ &= \frac{1}{(2\pi)^2} \int\int S(k_x, k_y, x', y', z') H(k_x, k_y, z') \mathrm{e}^{-\mathrm{i}k_x x} \mathrm{e}^{-\mathrm{i}k_y y} \, \mathrm{d}k_x \, \mathrm{d}k_y. \end{aligned} \tag{2}$$

The *medium filter* $H(k_x, k_y, z')$ represents the filtering action of the medium; $H(k_x, k_y, z')$ for homogeneous and layered media are specified in the appendix. Note that the depth z' of the source must be known to evaluate the medium filter; hence z' affects the observed potential $\phi(x, y, x', y', z')$ through $H(k_x, k_y, z')$.

2.3. Effect of source lateral location

The effect of lateral position (x', y') of the source is as follows. In the spatial frequency domain, shifting the source function in x by an amount x' becomes multiplication by $\mathrm{e}^{-jk_x x'}$, and similarly for y. If the source were actually located at the surface of the volume conductor, so that $z' = 0$, then the relation between the known function $s(x, y)$ and the actual source potential $s(x, y, x', y', 0)$ in the wavenumber domain would be

$$S(k_x, k_y, x', y', 0) = S(k_x, k_y) \mathrm{e}^{-\mathrm{i}k_x x'} \mathrm{e}^{-\mathrm{i}k_y y'} \tag{3}$$

Combining the effects of depth z' and lateral location (x', y') of the source on the Fourier transform of the observed potential $\Phi(k_x, k_y, x', y', z')$ yields

$$\Phi(k_x, k_y, x', y', z') = H(k_x, k_y, z') \mathrm{e}^{-\mathrm{i}k_x x'} \mathrm{e}^{-\mathrm{i}k_y y'} S(k_x, k_y) \tag{4}$$

which relates the observed potential $\Phi(k_x, k_y, x', y', z')$ to the known functional form $S(k_x, k_y)$ of the source. The problem is now to estimate the unknown location parameters (x', y', z').

3. Estimation of the location of a single source

Equation (4) shows that the filtering interpretation of the volume conductor has transformed the location estimation problem into a signal parameter estimation problem. The solution to these types of problems has been extensively studied and is well understood. In general, the maximum likelihood estimate of a parameter vector $\boldsymbol{A}$ in a signal $s(t, \boldsymbol{A})$ given noisy observations $r(t)$ of $s(t, \boldsymbol{A})$ plus additive white Gaussian noise of strength $N_0/2$ is found by maximising

$$\ln \Lambda[r(t), \boldsymbol{A}] = \frac{2}{N_0} \int_0^T r(t) s(t, \boldsymbol{A}) \, \mathrm{d}t - \frac{1}{N_0} \int_0^T s^2(t, \boldsymbol{A}) \, \mathrm{d}t \tag{5}$$

over the vector space spanned by $\boldsymbol{A}$ [6]. In the present problem, Parseval's theorem transforms the spatial integrations over x and y into wavenumber integrations over k_x and k_y, so that equation (5) becomes

$$\begin{aligned} \ln \Lambda[R(k_x, k_y), (x', y', z')] &= \frac{2}{N_0} \int_{-\infty}^{\infty} \int_{-\infty}^{\infty} R(k_x, k_y) S(k_x, k_y) H(k_x, k_y, z') \mathrm{e}^{-\mathrm{i}(k_x x' + k_y y')} \, \mathrm{d}k_x \, \mathrm{d}k_y \\ &\quad - \frac{1}{N_0} \int_{-\infty}^{\infty} \int_{-\infty}^{\infty} |S(k_x, k_y)|^2 H^2(k_x, k_y, z') \, \mathrm{d}k_x \, \mathrm{d}k_y . \end{aligned} \tag{6}$$

which is to be maximised over the location vector (x', y', z'). Note that in the second term the magnitude of the translation term is unity, so that it may be omitted; also, the strength $N_0/2$ of the observation noise is irrelevant. Here $R(k_x, k_y)$ is the Fourier transform of noisy observations of the potential at the surface of the volume conductor; in the noiseless case $R(k_x, k_y) = \Phi(k_x, k_y, x', y', z')$.

4. Estimation of the number and locations of multiple sources

To extend the results of the previous section to the case of multiple sources at various possible known depths, the parameter estimation algorithm must be augmented with a composite multiple-hypothesis test [6]. This is a case of significant interest in cardiology (see section 1).

4.1. Assumptions

To formulate the problem, we assume the following.

1. Sources can only exist at certain known depths z_i, with unknown location (x_i', y_i') at each depth. If a source exists at depth z_i, the ith layer is said to be 'active'. Sources may exist at some or all of the possible depths z_i.

2. If a source exists at a particular depth, its orientation is known (the method can be extended to sources with unknown orientation; see section 5).

3. The *a priori* probability that the ith layer is active is 0.5. This implies that the number of active layers will be a binomial distribution with mean $N/2$, which is reasonable; without this assumption the problem involves much more computation (though it can still be solved). The event that the ith layer is active is independent of the event that the jth layer is active.

4. The goal is to minimise the probability of error in choosing the active layers, while computing the maximum likelihood estimates of the locations of the source in each active layer.

Now the problem can be formulated as a composite multiple-hypothesis minimum-error probability test, with each hypothesis corresponding to a particular combination of active depths. This means that for each hypothesis, the locations of the sources are estimated, and then the most likely hypothesis given the estimates is chosen. If there are N possible active layers, then there are 2^N hypotheses.

4.2. Likelihood function for multiple sources

Equation (6) is based on the use of equation (2) to compute the observed potential due to a single source. Since the medium is assumed to be linear, superposition can be used to extend equation (2) to multiple sources. Then the observed potential $\phi(x, y)$ at the surface of the volume conductor due to N active layers (i.e. N sources $\{S_i(k_x, k_y, x_i', y_i', z_i), i = 1, \ldots, N\}$ at depths $\{z_i, i = 1, \ldots, N\}$) is given by:

$$\phi(x, y) = \mathcal{F}^{-1}_{k_x \to x} \mathcal{F}^{-1}_{k_y \to y} \sum_{i=1}^{N} S_i(k_x, k_y, x_i', y_i', z_i) H(k_x, k_y, z_i) \tag{7}$$

where N is the number of sources and (x_i', y_i', z_i) is the location of the ith source. Note that $\phi(x, y)$ depends implicitly on $\{(x_i', y_i', z_i), i = 1, \ldots, N\}$; however, we do not explicitly indicate this dependence.

Let $H_{i_1, i_2, \ldots, i_N}$, $i_j = 0$ or 1, represent the hypothesis that the layers corresponding to $i_j = 1$ are active. By assumption 3 these hypotheses will be equally likely *a priori*. Let $\{(x_j', y_j', z_j), i_j = 1\}$ be the locations of the active sources, and let $R(k_x, k_y)$ be the Fourier transform of noisy observations of $\phi(x, y)$. Then the log-likelihood function for minimum-error probability detection with equal *a priori* probabilities can be found by inserting the right-hand side of equation (7) into equation (6). The result is:

$$\begin{aligned} \ln \Lambda[R(k_x, k_y)] = {} & \frac{2}{2^N N_0} \int_{-\infty}^{\infty} \int_{-\infty}^{\infty} R(k_x, k_y) \sum_{n: i_n = 1} S_n(k_x, k_y) H(k_x, k_y, z_n) \\ & \times \mathrm{e}^{-\mathrm{i}(k_x x_n' + k_y y_n')} \, \mathrm{d}k_x \, \mathrm{d}k_y \\ & - \frac{1}{2^N N_0} \int_{-\infty}^{\infty} \int_{-\infty}^{\infty} \left| \sum_{n: i_n = 1} S_n(k_x, k_y) H(k_x, k_y, z_n) \right. \\ & \left. \times \mathrm{e}^{-\mathrm{i}(k_x x_n' + k_y y_n')} \right|^2 \mathrm{d}k_x \, \mathrm{d}k_y. \end{aligned} \tag{8}$$

For each of the 2^N sets of $\{i_1, \ldots, i_N\}$, this is maximised over $\{(x_j', y_j'), i_j = 1\}$ (recall that the depths z_i are all known *a priori*). Then the maximum of the resulting 2^N numbers is found; the corresponding hypothesis $H_{i_1, i_2, \ldots, i_N}$ denotes which layers are active. The previously computed locations $\{(x_j', y_j'), i_j = 1\}$ for that hypothesis then denote the locations of the source in each active layer.

5. Estimation of source orientations

Given knowledge of the functional form (and implicitly the orientation) of bioelectric sources at unknown locations, their presence and locations can be estimated as above. This can be extended to estimation of additional parameters for the sources; for example, their functional forms can be parametrised, and the unknown parameters estimated as was the location above. In this section we extend the above results to include *orientation* of the source as an additional parameter to be estimated.

We consider the single-source case first, so that we have a single source at unknown location (x', y', z') at an unknown orientation θ. Since the two-dimensional Fourier transform of a rotation in the spatial domain is an identical rotation in the frequency domain, the Fourier transform $\Phi(k_x, k_y, x', y', z', \theta)$ of the observed potential is:

$$\Phi(k_x, k_y, x', y', z', \theta) = H(k_x, k_y, z')\mathrm{e}^{-\mathrm{i}k'_x x'}\mathrm{e}^{-\mathrm{i}k'_y y'} S(k'_x, k'_y) \tag{9}$$

where $[k'_x, k'_y]$ is $[k_x, k_y]$ rotated by angle θ, so that

$$k'_x = k_x \cos\theta + k_y \sin\theta \qquad k'_y = -k_x \sin\theta + k_y \cos\theta. \tag{10}$$

Note that $H(k_x, k_y, z')$ is invariant under rotation (see appendix A). Substituting this into equation (6) results in

$$\begin{aligned}\ln \Lambda[R(k_x, k_y), (x', y', z', \theta)] &= \frac{2}{N_\mathrm{o}} \int_{-\infty}^{\infty}\int_{-\infty}^{\infty} R(k_x, k_y) S(k_x \cos\theta + k_y \sin\theta, -k_x \sin\theta + k_y \cos\theta) \\ &\quad \times H(k_x, k_y, z')\mathrm{e}^{-\mathrm{i}x'(k_x\cos\theta + k_y \sin\theta) - \mathrm{i}y'(k_y\cos\theta - k_x\sin\theta)}\,\mathrm{d}k_x\,\mathrm{d}k_y \\ &\quad - \frac{1}{N_\mathrm{o}} \int_{-\infty}^{\infty}\int_{-\infty}^{\infty} |S^2(k_x \cos\theta + k_y \sin\theta, -k_x \sin\theta + k_y \cos\theta)| \\ &\quad \times H^2(k_x, k_y, z')\,\mathrm{d}k_x\,\mathrm{d}k_y. \end{aligned} \tag{11}$$

which is maximised over (x', y', z', θ). Note that in the second term the magnitude of the translation term is unity, so that it may be omitted. Also note that this method can be extended in a straightforward manner to the case of multiple active sources, as in section 4.2.

6. Numerical results

To evaluate the new technique, several numerical simulations were performed. The 'measurements' were simulated using the medium filter formulation of [4, 5], using the test cardiac action potentials of [4, 5], which is a two-dimensional version of the test action potential given in [11]. These action potentials are of larger spatial extent than could be observed at a single instant; the method of sequential sampling, discussed in [4, 5], allows the entire action potential to be observed. This technique works unless the samples are taken along a line exactly parallel to the direction of propagation of the action potential; as long as there is a non-zero component along the sampling line the technique works.

The following example problems were simulated.

1. Estimation of location of a single action potential with known orientation.
2. Estimation of number and locations of active layers.
3. Estimation of location and orientation of a single action potential.

All measurements were made in homogeneous tissue with isotropic conductivity. The simulated measurements included additive white Gaussian noise, at signal-to-noise ratios of 20, 10, 6, 3 and 0 dB. All integrals were evaluated using the trapezoidal rule. The 2D Fourier transforms were computed using a 256 × 256 discrete Fourier transform, zero-padded to prevent aliasing.

In the matched filter expressions, the following crude estimate of the functional form of the unknown sources was used:

$$s(x, y) = \mathrm{rect}(s_x, s_y, V_{\mathrm{RMS}}). \tag{12}$$

Here $\mathrm{rect}(s_x, s_y, V_{\mathrm{RMS}})$ is a two-dimensional rectangular pulse of spatial extent s_x by s_y, and amplitude V_{RMS}. Even though this function represents a gross approximation to the functional form of the unknown sources, it proved to be quite effective. This fortunate result can be explained by noting that the matched filter expressions weight the lower spatial frequencies of the measurements more heavily than the higher spatial frequencies, since the higher frequencies are more severely attenuated by the volume conductor (and are therefore more severely corrupted by noise). Since the primary differences between this model and the actual source potentials are restricted to relatively high spatial frequencies, a more accurate model would provide limited improvement.

Example 1. The form of the action potential is shown in figure 1. This potential was shifted by an unknown translation; only its spatial extent $s_x = 20$ cm, $s_y = 2$ cm, the RMS voltage $V_{\mathrm{RMS}} = -50$ mV, and the fact that there was only one action potential, were known to the algorithm. Results are given in table 1.

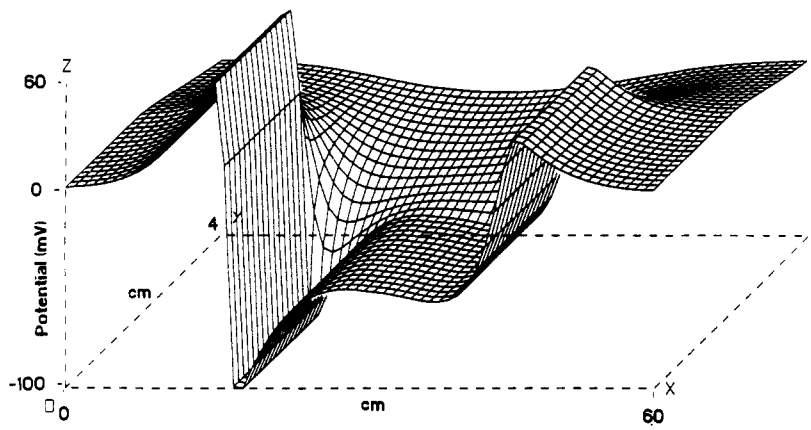

Figure 1. The two-dimensional test function used as a source potential for all the simulated experiments. The region $0 < y < 2$ cm is representative of the extracellular potential induced by activated cardiac muscle. The region 2 cm $< y <$ 4 cm represents inactive tissue.

Table 1.

SNR	Actual (x', y', z') (cm, cm, mm)	Estimated (x', y', z') (cm, cm, mm)
20	2.0, 4.0, 5.0	2.0, 4.0, 5.0
10	2.0, 4.0, 5.0	2.0, 4.0, 5.2
6	2.0, 4.0, 5.0	2.1, 3.8, 5.4
3	2.0, 4.0, 5.0	2.6, 3.2, 6.1
0	2.0, 4.0, 5.0	3.4, 2.4, 7.3

Note that performance degrades with increasing noise, as expected. The threshold is at a signal-to-noise ratio of about 4 dB; performance degrades rapidly below this point.

We now discuss the Cramer–Rao lower bound for the variance of any unbiased estimator $\hat{z}$ for the depth z of the source. We assume additive white Gaussian noise with strength N, and a homogeneous medium. Using equation (2), and the homogeneous medium filter from appendix A, the Cramer–Rao bound is easily shown to be (see [6])

$$E[(z-\hat{z})^2] \geq 2\pi^2 N \left(\int_0^{\infty} \int_0^{2\pi} k^3 \mathrm{e}^{-2kz} |S(k,\phi)|^2 \, \mathrm{d}\phi \, \mathrm{d}k \right)^{-1} \tag{13}$$

where $\hat{z}$ is the estimate of depth z, $k = (k_x^2 + k_y^2)^{1/2}$ is the radial wavenumber, and $S(k, \phi)$ is the Fourier transform of the source potential in polar coordinates.

The Cramer–Rao bound for depth illustrates several interesting points.

1. As depth z increases, the weighting factor e^{-2kz} decreases exponentially. Although this factor is inside the integral, this accounts for the presence of a performance threshold, and the rapid degradation of performance beyond it.

2. The low-wavenumber components of the source potential are important, due to the factor of e^{-2kz}, which attenuates high-wavenumber components of the source potential. This can also be seen in the likelihood function (6), in which the data are weighted by the medium filter $H = \mathrm{e}^{-kz}$. This is reasonable, since these components are strongly attenuated by the medium, so that they are weaker relative to the noise.

3. However, very low-wavenumber components in the source potential are not helpful, due to the factor of k^3, which attenuates very low-wavenumber components. This is reasonable since the medium has little effect on these components, so that they are less useful in estimating the depth z.

Of course, mean-square error in depth estimation is not necessarily an appropriate measure of performance. Also, the Cramer–Rao bound is heavily dependent on the source potential characteristics. For these reasons, we believe a numerical comparison of the above results with the Cramer–Rao bound is not appropriate.

Example 2. Action potentials of the form shown in figure 1 were located at two of five possible depths. The possible depths were 1, 2, 3, 5 and 8 mm below the surface; the actual active layers were 3 and 5 mm below the surface. For a signal-to-noise ratio of greater than SNR = 3, the algorithm correctly picked out the two active layers; the unknown lateral locations of the two active layers were estimated as shown in table 2.

Again the location estimation performance degrades with increasing noise, although the active layers were correctly determined in all cases with a signal-to-noise

Table 2.

	Actual (x', y') (cm, cm)		Estimated (x', y') (cm, cm)	
SNR	3 mm layer	5 mm layer	3 mm layer	5 mm layer
20	2.0, 4.0	1.0, 3.0	2.0, 4.0	1.0, 3.0
10	2.0, 4.0	1.0, 3.0	2.2, 4.1	1.2, 3.1
6	2.0, 4.0	1.0, 3.0	2.4, 4.3	1.5, 3.4
3	2.0, 4.0	1.0, 3.0	3.0, 5.4	2.1, 4.3

ratio of greater than SNR = 3. For SNR = 0, the algorithm incorrectly picked out two additional active layers, specifically, the 1 and 2 mm layers. This makes evaluation for negative signal-to-noise ratios difficult.

Example 3. Here example 1 was augmented with an unknown orientation of the action potential. Results are shown in table 3.

Table 3.

SNR	Actual (x', y', z', θ) (cm, cm, mm, deg)	Estimated (x', y', z', θ) (cm, cm, mm, deg)
20	2.0, 4.0, 5.0, 45	2.0, 4.0, 5.0, 45
10	2.0, 4.0, 5.0, 45	2.2, 4.3, 5.2, 45
6	2.0, 4.0, 5.0, 45	2.4, 3.7, 5.5, 56
3	2.0, 4.0, 5.0, 45	2.9, 3.4, 5.9, 63
0	2.0, 4.0, 5.0, 45	3.4, 3.3, 6.2, 63

Note that the necessity of estimating an additional parameter degrades the location estimates from those of example 1.

7. Conclusions

An algorithm for the estimation of the number and locations of bioelectric sources in a horizontally layered volume conductor was presented. By modelling the extracellular medium as an equivalent filter, the location estimation problem was transformed into one of estimating parameters of this equivalent filter, given cursory knowledge of the functional form of the desired sources. The algorithm was shown to be effective even using a crude rectangular pulse estimate of the functional forms of the bioelectric sources; hence these functional forms need not be known *a priori*. The algorithm implements the matched filter in the spatial frequency domain; the data processing consists of a 2D Fourier transform.

In principle, this approach could be extended to the computation of additional source potential parameters other than location and orientation. Unknown orientation could be added to the multiple active layer problem; source parameters such as rise time can also be estimated. However, performance is degraded as the number of parameters to be estimated increases (compare examples 1 and 3). The *a priori* probabilities of various layers being active can be assigned arbitrarily. This results in a straightforward generalisation of equation (6) (see [6]); however, this increases the computation substantially.

Appendix A

The medium filters for extracellular potentials are as follows [4, 5].

Homogeneous media

For a homogeneous medium, the medium filter $H(k_x, k_y, z)$ is given by

$$H(k_x, k_y, z) = \mathrm{e}^{-(k_x^2+k_y^2)^{1/2}z} \tag{A1}$$

as in [4].

This is the solution of Laplace's equation that satisfies the boundary conditions of agreeing with a specified source function on the plane $z = 0$ and decaying to zero at infinity. The two-dimensional Fourier transform of the potential observed at the surface of a volume conductor due to a source at depth z' is then

$$\Phi(k_x, k_y, z') = \mathrm{e}^{-(k_x^2+k_y^2)^{1/2}z'} S(k_x, k_y) \tag{A2}$$

where $S(k_x, k_y)$ is the two-dimensional Fourier transform of the source potential.

Note that $H(k_x, k_y, z)$ is a low-pass spatial filter whose attenuation increases exponentially with increasing distance and/or spatial frequency. Hence the effect of the volume conductor is to attenuate and smooth the source potential, so that the higher spatial frequency components of the source potential are most severely corrupted by measurement noise. Consequently, regularisation in the form of low-pass filtering of the solution of the inverse problem of determining the source potential from the observed potential is required.

Layered media

For layered media, the medium filter $H(k_x, k_y, z)$ is given by

$$H(k_x, k_y, z) = A_n \mathrm{e}^{-(k_x^2+k_y^2)^{1/2}z} + B_n \mathrm{e}^{+(k_x^2+k_y^2)^{1/2}z} \tag{A3}$$

where A_n and B_n are functions of spatial frequency and are different in each layer of different conductivity. Using continuity of normal current density and voltage at each interface between layers, the A_n and B_n in adjoining layers are related by [5]

$$\begin{bmatrix} A_{n-1} \\ B_{n-1} \end{bmatrix} = \left(\frac{\sigma_n}{\sigma_{n-1}}\right)^{1/2} \frac{1}{(1+\Gamma_n^2)^{1/2}} \begin{bmatrix} 1 & a_n\Gamma_n \\ \Gamma_n/a_n & 1 \end{bmatrix} \begin{bmatrix} A_n \\ B_n \end{bmatrix} \tag{A4}$$

$$\Gamma_n = \frac{\sigma_n - \sigma_{n+1}}{\sigma_n + \sigma_{n+1}} \qquad a_n = \mathrm{e}^{2(k_x^2+k_y^2)^{1/2}z_n} \tag{A5}$$

where σ_n and z_n are the conductivity and thickness, respectively, of the nth layer. Conductivity discontinuities also result in attenuation of high spatial frequency components (smoothing) of the source potential. This is in addition to that induced by each layer itself.

These filters relate the extracellular potential at the surface of an active structure to the extracellular potential in the surrounding medium.

Appendix B

The medium filters relating transmembrane potentials to surface evoked extracellular potentials are as follows.

We make the following assumptions as in [9, 13].

1. The membrane is thin relative to the dimensions of the equivalent cell and the external media.
2. The extracellular potential is the result of an impressed current density, normal to the membrane.
3. The normal current density across the membrane is continous.

The potentials on the inner and outer surface of the membrane are induced and related by the impressed current density. Therefore expressions for the medium filters for the regions both above and below the membrane are required.

At the conducting boundary the normal current density is continous. Hence for a membrane at $z = a$

$$\sigma_{\mathrm{i}} \left.\frac{\partial \Phi_{\mathrm{i}}(k_x, k_y, z)}{\partial z}\right|_{\rho=a} = \sigma_{\mathrm{o}} \left.\frac{\partial \Phi_{\mathrm{o}}(k_x, k_y, z)}{\partial z}\right|_{\rho=a} \tag{B1}$$

where Φ_{i} is the potential in the medium below the membrane, Φ_{o} is the potential in the medium above the membrane, σ_{i} is the conductivity immediately below the membrane, and σ_{o} is the conductivity immediately above the membrane.

Let Φ_{si} be the potential at the inner surface of the membrane, Φ_{so} be the potential at the outer surface of the membrane, H_{i} be the medium filter for the region below the membrane, and H_{o} be the medium filter for the region above the membrane. Note that $\Phi_{\mathrm{i}} = H_{\mathrm{i}}\Phi_{\mathrm{si}}$ and $\Phi_{\mathrm{o}} = H_{\mathrm{o}}\Phi_{\mathrm{so}}$, and that Φ_{si} and Φ_{so} are not functions of depth z (the depth dependence is contained in H_{i} and H_{o}). Then the interface current continuity relation (B1) can be rewritten as

$$\sigma_{\mathrm{i}} \left.\frac{\partial \Phi_{\mathrm{si}}(k_x, k_y) H_{\mathrm{i}}(k_x, k_y, z)}{\partial z}\right|_{\rho=a} = \sigma_{\mathrm{o}} \left.\frac{\partial \Phi_{\mathrm{so}}(k_x, k_y) H_{\mathrm{o}}(k_x, k_y, z)}{\partial z}\right|_{\rho=a} \tag{B2}$$

Then the *transmembrane potential*, defined as $\Phi_{\mathrm{mem}}(k_x, k_y) = \Phi_{\mathrm{si}}(k_x, k_y) - \Phi_{\mathrm{so}}(k_x, k_y)$, is related to the potential at the outer surface of the membrane by

$$\begin{aligned}\Phi_{\mathrm{so}}(k_x, k_y) &= \Phi_{\mathrm{mem}}(k_x, k_y) \frac{-\sigma_{\mathrm{i}}(\partial H_{\mathrm{i}}(k_x, k_y, z)/\partial z)|_{z=a}}{\sigma_{\mathrm{o}}(\partial H_{\mathrm{o}}(k_x, k_y, z)/\partial z)|_{z=a} + \sigma_{\mathrm{i}}(\partial H_{\mathrm{i}}(k_x, k_y, z)/\partial z)|_{z=a}} \\ &= \Phi_{\mathrm{mem}}(k_x, k_y) H_{\mathrm{mem}}(k_x, k_y).\end{aligned} \tag{B3}$$

Thus if bioelectric sources are modelled as transmembrane potentials, rather than extracellular potentials, $H(k_x, k_y, z)$ from appendix A should be multiplied by $H_{\mathrm{mem}}(k_x, k_y)$ throughout.

Appendix C

The medium filters relating current source densities to surface evoked extracellular potentials are as follows.

Using the assumptions of the previous appendix, the impressed current density in the membrane is related to the potential in the extracellular medium by:

$$J_i(k_x, k_y) = -\sigma_o \left. \frac{\partial \Phi_o(k_x, k_y, z)}{\partial z} \right|_{z=a} \tag{C1}$$

where J_i is the impressed current density, assumed to be normal to the membrane.

Since the extracellular potential is related to the potential at the surface of the membrane by the extracellular medium filter from appendix A, this becomes

$$J_i(k_x, k_y) = -\sigma_o \left. \frac{\partial \Phi_{so}(k_x, k_y) H_o(k_x, k_y, z)}{\partial z} \right|_{z=a} \tag{C2}$$

so that the filter relating the potential at the surface of the membrane to the impressed current density is

$$\Phi_{so}(k_x, k_y) = \frac{-J_i(k_x, k_y)}{(-\sigma_o(\partial H_o(k_x, k_y, z)/\partial z)|_{z=a})} = J_i(k_x, k_y) H_{curr}(k_x, k_y). \tag{C3}$$

Thus if bioelectric sources are modelled as current source densities, rather than extracellular potentials, $H(k_x, k_y, z)$ from appendix A should be multiplied by $H_{curr}(k_x, k_y)$ throughout.

References

[1] Di Persio D A and Barr R C 1987 A prototype inverse solution in one dimension to find the origin of excitration, strand radius, intracellular resistivity, or distance from the surface *IEEE Trans. Biomed. Eng.* **BME-34** 681–90

[2] Oostendorp T F and Van Oosterom A 1989 Source parameter estimation in inhomogeneous volume conductors of arbitrary shape *IEEE Trans. Biomed. Eng.* **BME-36** 382–91

[3] Gabor D and Nelson C V 1954 Determination of the resultant dipole of the heart from measurements on the body surface *J. Appl. Physiol.* **25** 413–22

[4] Xydis T G, Yagle A and Kadish A 1990 A filtering approach to the two-dimensional volume conductor forward and inverse problems *IEEE Trans. Biomed. Eng.* submitted

[5] Xydis T G, Yagle A and Kadish A 1990 Bioelectric potential propagation through layered two-dimensional volume conductors *IEEE Trans. Biomed. Eng.* submitted

[6] Van Trees H L 1968 *Detection, Estimation, and Modulation Theory* part 1 (New York: Wiley)

[7] Spach M S, Miller W T III, Miller-Jones E, Warren R B and Barr R C 1979 Extracellular potentials related to intracellular action potentials during impulse conduction in anisotropic canine cardiac muscle *Circulation Res.* **45** 356–71

[8] Ganapathy N, Clark J W, Wilson O B and Giles W 1985 Forward and inverse potential field solutions for cardiac strands of cylindrical geometry *IEEE Trans. Biomed. Eng.* **BME-32** 566–77

[9] Clark J W and Plonsey R 1966 A mathematical evaluation of the core conductor model *Biophys. J.* **6** 95–112

[10] Plonsey R 1969 *Bioelectric Phenomena* (New York: McGraw-Hill)

[11] Harmon T L, Liebfried T F, Clark J W and Hibbs C W 1975 A comparison of two methods for determining the extracellular potential field of an isolated Purkinje strand in a volume conductor *IEEE Trans. Biomed. Eng.* **BME-22** 174–83

[12] Heringa A, Stegeman D F, Uijen G J H and J P C de Weerd 1982 Solution methods of electrical field problems in physiology *IEEE Trans. Biomed. Eng.* **BME-29** 34–42

[13] Geselowitz D B 1966 Comments on the core conductor model *Biophys. J.* **6** 691–2